applied sciences

MDPI

Article

Specific Modeling Issues on an Adaptive Winglet Skeleton

Salvatore Ameduri [1], Ignazio Dimino [1,*], Antonio Concilio [1], Umberto Mercurio [2] and Lorenzo Pellone [2]

[1] Department of Adaptive Structures, The Italian Aerospace Research Centre (CIRA), Via Maiorise, 81043 Capua, Italy; s.ameduri@cira.it (S.A.); a.concilio@cira.it (A.C.)
[2] Department of Aeronautical Technologies Integration, The Italian Aerospace Research Centre (CIRA), Via Maiorise, 81043 Capua, Italy; u.mercurio@cira.it (U.M.); l.pellone@cira.it (L.P.)
* Correspondence: I.Dimino@cira.it

Abstract: Morphing aeronautical systems may be used for a number of aims, ranging from improving performance in specific flight conditions, to keeping the optimal efficiency over a certain parameters domain instead of confining it to a single point, extending the flight envelope, and so on. An almost trivial statement is that traditional skeleton architectures cannot be held as a structure modified from being rigid to deformable. That passage is not simple, as a structure that is able to be modified shall be designed and constructed to face those new requirements. What is not marginal, is that the new configurations can lead to some peculiar problems for both the morphing and the standard, supporting, elements. In their own nature, in fact, adaptive systems are designed to contain all the parts within the original geometry, without any "external adjoint", such as nacelles or others. Stress and strain distribution may vary a lot with respect to usual structures and some particular modifications are required. Sometimes, it happens that the structural behavior does not match with the common experience and some specific adjustment shall be done to overcome the problem. What is reported in this paper is a study concerning the adaptation of the structural architecture, used to host a winglet morphing system, to make it accomplish the original requirements, i.e., allow the deformation values to be under the safety threshold. When facing that problem, an uncommon behavior of the finite element (FE) solver has been met: the safety factors appear to be tremendously dependent on the mesh size, so as to raise serious questions about the actual expected value, relevant for the most severe load conditions. On the other side, such singularities are more and more confined into single points (or single lines), as the mesh refines, so to evidence somehow the numerical effect behind those results. On the other side, standard engineering local methods to reduce the abovementioned strain peaks seem to work very well in re-distributing the stress and strain excesses to the whole system domain. The work does not intend to give an answer to the presented problem, being instead focused on describing its possible causes and its evident effects. Further work is necessary to detect the original source of such inconsistencies, and propose and test operative solutions. That will be the subject of the next steps of the ongoing research.

Keywords: adaptive structures; FE modeling; stress analysis; loads assessment

Citation: Ameduri, S.; Dimino, I.; Concilio, A.; Mercurio, U.; Pellone, L. Specific Modeling Issues on an Adaptive Winglet Skeleton. *Appl. Sci.* **2021**, *11*, 3565. https://doi.org/10.3390/app11083565

Academic Editor: Ruxandra Mihaela Botez

Received: 16 March 2021
Accepted: 12 April 2021
Published: 15 April 2021

1. Introduction

The long experience gained by an extended Italian group on morphing, developed from more than 20 years of activity in international contexts, led to the ambitious aim of proposing a project concerning the design and realization of a complete morphing wing implementing different kinds of devices in its basic geometry. The occasion matured within the CS2 GRA frame, as Leonardo S.p.A. (Aircraft Division) issued a call for proposals on several topics, among which the abovementioned subjects [1]. CIRA, University of Napoli, and Politecnico di Milano took charge of designing and realizing four different adaptive prototypes to be installed on a single wing: a winglet, an adaptive trailing edge, and an adaptive leading edge plus an adaptive wingtip, respectively. The project did rely at a

wide extent on the further development of numerical capabilities particularly suited for morphing system design, on the wake of the developed expertise.

Kinematic systems differ from compliant morphing systems, as their basic architecture is almost an extension of standard devices already placed on any kind of aircraft, such as flap, slats, and so on, while the latter tries to modify the inner structure of the reference craft to make it suitably deformable [2–6]. In both cases, however, the need of assigning further macroscopic degrees of freedom to the target structure, imposes the creation of high-nodal density models [7]. They have to consider the deployment of a more complex and articulated structural outline, an immediate consequence of the additional mobility and the increased number of parts.

These kinds of models have been reported in the literature to be characterized by a certain behavior with respect to further increase of their density [8–11]. As the number of nodes and elements increase, or conversely, the mesh step decreases, certain singularities are shown that turn on the debate among the researchers about the fact they are actual index of a physical behavior or instead are simply linked to some mathematical issue [12]. The fact is, revealing the point deformation in a very limited geometry domain is a true challenge considering that standard sensors, even when miniaturized, only produce information along a certain area and do not have the capability of providing point information. Of course, this can be limitedly true for displacements, while they may have a dramatic impact on strain detection [13,14].

In light of these considerations, the paper herein presented reports some significant experiences that the authors believe to be interesting to discuss, concerning specifically the increasingly higher modal density mesh effects on the structural response. This goal had an even more significance, because of the possibility of attaining a wide database of experimental output, as the target element did undergo an extensive test campaign. As introduced, lab acquisitions were not expected to allow a deeper correlation among experimental and numerical data, but it was considered that could at least make a base of reference, even for further activities.

As part of the Clean Sky 2 program, CIRA is the leader of the AIRGREEN2 project in the REG-IADP platform whose leader is Leonardo S.p.A. (Aircraft Division). The AIRGREEN2 project began in November 2015 and will end in 2023. The main purpose of the project is the development and validation of technologies suitable for the wing of the future regional aircraft of LDO and related demonstrators up to, for some of them, validation by experimentation in flight. The technological strands that characterize the AIRGREEN2 project are:

Innovative wing structure (design, manufacturing and testing): innovative composite design, repair, structural health monitoring, LRI (liquid resin infusion) processes and AFP (automatic fiber placement) [15,16].

Innovative aerodynamic design: extended laminar flow, 3D riblets, morphing winglet, morphing flap to stay in condition of maximum aerodynamic efficiency during the cruise, development of techniques for load control and alleviation (LCA system based on an innovative wing tip and morphing winglet) [17].

Adaptivity: high lift performance using an innovative leading edge (droop nose) compatible with laminarity requirements and coupled to Morphing Flap

In line with the main targets of AIRGREEN2, specific morphing concepts have been being under investigation [1]. They will contribute to enhance the performance of the A/C, to optimize the load distribution on the wing structure and to increase the lift generation.

Four different concepts have been conceived:

(1) An adaptive leading edge, able to increase its curvature, to generate the so called droop nose effect [18]. The smooth morphed geometry dramatically contributes to the lift generation capability at specific operational conditions (take-off and landing), while the absence of geometric discontinuities in clean configuration cooperates in keeping the laminar flow in cruise. The device is constituted by a compliant internal

structure, moved by a spanwise torque actuator. The deformation is then transmitted to the surrounding skin, a carbon fiber laminate.

(2) A multifunctional flap, relying upon an adequate number of degrees of freedom (DOFs) to change its curvature, through a finger-like kinematic architecture [19]. The role of the device is to cooperate with the adaptive leading edge to generate additional lift (change of the curvature along the entire chord in fully extracted configuration) and to enhance the aerodynamic efficiency and optimize the load distribution (deflection of the aft tabs in fully retracted configuration).

(3) An adaptive wing tip, a 1 DOF aerodynamic movable surface mounted at the tip of the wing [20]. Deflected by an electromechanical actuator, its role is to cooperate with the multifunctional flap in the load control and alleviation operations.

(4) An adaptive winglet, mounted alternatively to the just mentioned wing tip and constituted by a fixed structure equipped with independent movable surfaces [21,22]. The scope is to adaptively alter the load distribution along the wing span to increase the aerodynamic performance, from one side, and to alleviate the stress level, from the other side.

The novelty of aforementioned devices is different for each of them. Adaptive trailing edges are very popular in literature and different architectures and concepts may be found in bibliography. The main characteristics of the one herein reported, and originally developed by the University of Napoli "Federico II", stands in its capability of combining up to three modalities of morphing (classical flap-like modification, tab-like movement, and artificial chord-extension), while keeping low the number of parts and therefore its complexity. The adaptive winglet developed by CIRA is almost an innovation itself, since the previous experiences on that topic mainly concern the introduction of a tab-like system, mainly vibrating at high frequencies in order to try gust effect alleviation strategies (Airbus Innovation Work, 2015), or introducing hinged wing tips for the modification of the configuration in-flight. In this case, the system is instead conceived to perform both static and dynamic functionalities along all the aircraft mission. It should be reminded that this kind of system shows the intrinsic challenge of implementing large weights at the extremity of the wing, therefore modifying intimately the aeroelastic behavior of reference aircraft.

The adaptive leading edge is characterized by an internal compliant architecture that cooperates with the external structure in absorbing loads and at the same time drives the deformation, leading to the drooped nose configuration. The device jointly to the multifunctional flap action leads to a significant hyper lift generation, moving upward the lift curve of the wing and increasing the stall angle.

The innovative wing tip due to its location on the wing and to its specific configuration is particularly prone to implementation of LCA strategies of new conception.

1.1. General Overview of the Winglet System

Among the just mentioned four AIRGREEN 2 morphing devices which may be considered for similar purposes, this study focuses on specific modeling issues addressed during the advanced design of a finger-like mechanism-based morphing winglet developed by CIRA. Such an integrated morphing system, capable to reduce wing-bending moments and increase aircraft flight stability in response to changing flight conditions, has proved to provide significant aerodynamic benefits, estimated on the order of 2.5% LoD at high CL with respect to the optimal passive winglet counterpart [23].

The morphing winglet system consists of two "finger-like" mechanisms realizing two independent morphing tabs moving both upward and downward. Such deflections are driven by dedicated electromechanical actuators [24]. One of the major advantages of this architecture is the capability to move the individual surfaces either synchronously or independently to different angles. This ensures smoother morphing winglet aeroshapes and a more efficient distribution of the span-wise aerodynamics, as estimated by computational fluid dynamics (CFD) simulations (Figure 1).

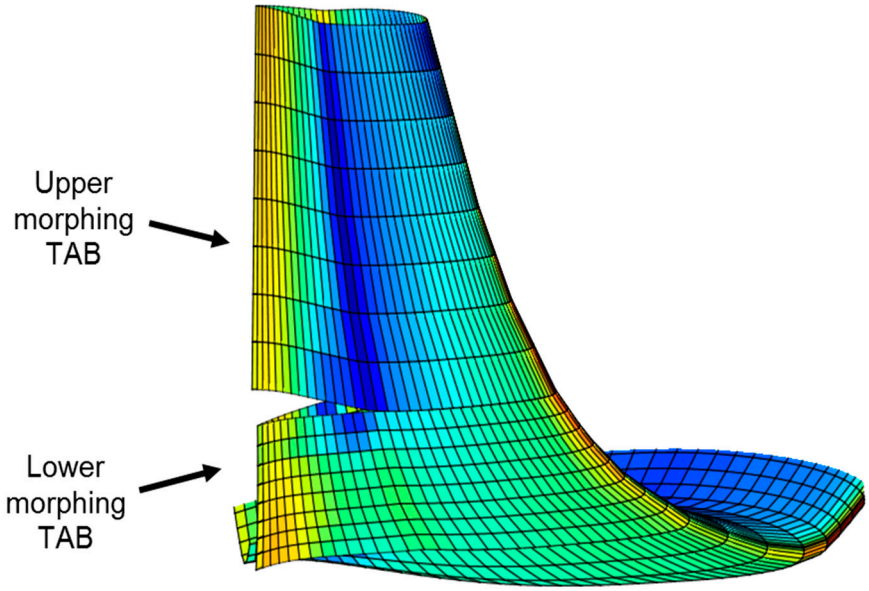

Figure 1. Morphing winglet concept with upper and lower control surfaces [24].

The structural layout of the morphing winglet consists of a passive and an active part [25]. The former is made of laminate skin panels and a torsion box consisting of spars and ribs. The latter incorporate two hinged mechanisms covered by a segmented skin. By means of linking rods, hinged on non-adjacent blocks, the morphing capability is enabled by the relative rotations of three adjacent blocks, which are free to rotate around the hinges on the camber line, thus physically turning the camber line into an articulated chain of consecutive segments. Each tab is, therefore, a single degree of freedom (SDOF) system; if rotation of any of the blocks is prevented, no change in shape can be obtained. On the contrary, if an actuator moves any of the blocks, all the other blocks follow the movement accordingly.

1.2. The Reference FE Model

For the purpose of this research, focus is given to the passive structure of the winglet, shown in Figure 2, sized to withstand the worst-case loading conditions that it is expected to experience in normal operation. The structural layout, consisting of upper and lower CFRP panels, internal CFRP spars and ribs, is overall modeled by 10,593 2D elements, defining a reference finite element (FE) model [23] considered in this study to investigate specific modeling issues.

Both the upper and lower skin panels consist of the same CFRP lay-up sequence represented by CQUAD4 and CTRIA3 elements in relation with laminate property entries (PCOMP) on the middle surface. All laminates are symmetric and are mainly composed of fabric layers. UD-plies in x direction are used for reinforcement. The material orientation is defined on the respective CQUAD4/CTRIA3 entry and is aligned along the span. All the elements used in the FE model are linear. The thickness of the laminates of the skins, spars and ribs is between 2.7 and 3.6 mm. The final weight of the complete structure is below the preliminary design target of 50 kg.

For the analysis of the laminates, a maximum/minimum strain criterion in 11- and 22-direction is used. Additionally, stress is also evaluated in 11-, 22- and 12-directions. The ply stresses and strains are read from the FEM results. The failure indexes for each ply were then calculated. The enveloped results were then elaborated to allow for computation of the minimum failure index.

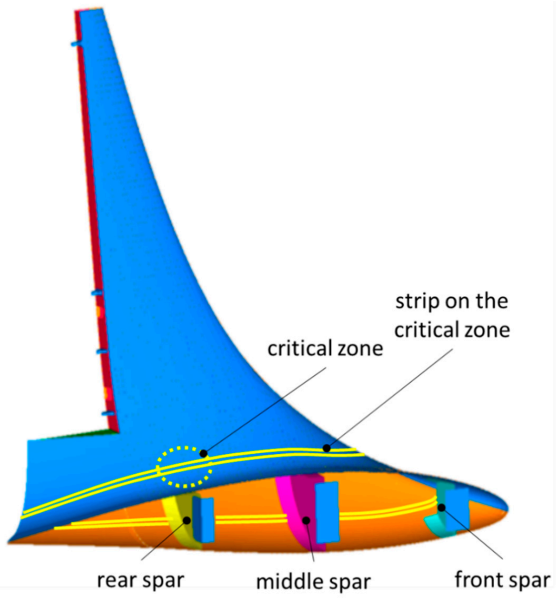

Figure 2. Finite element (FE) model of the winglet without the moveable surfaces [23].

1.3. Load System

Different load conditions have driven the design of the fixed part of the winglet, corresponding to the most severe solicitation at bending, torsion and shear, both in negative and positive directions. An initial trade-off has been carried out to estimate the impact of each load condition on the stress level generated into the main subparts of the structure. The radar plot, shown in Figure 3, illustrates a comparison of the stress produced by the just mentioned load cases, normalized with respect to the most severe case. As evident, the first load case, corresponding to the maximum bending in positive direction (inward deflection of the winglet) dramatically envelopes the other ones, followed by the load case 2, due to the bending too, but in the opposite direction. For this reason, only the 1st load case has been considered significant for the investigations illustrated in the next part of the work.

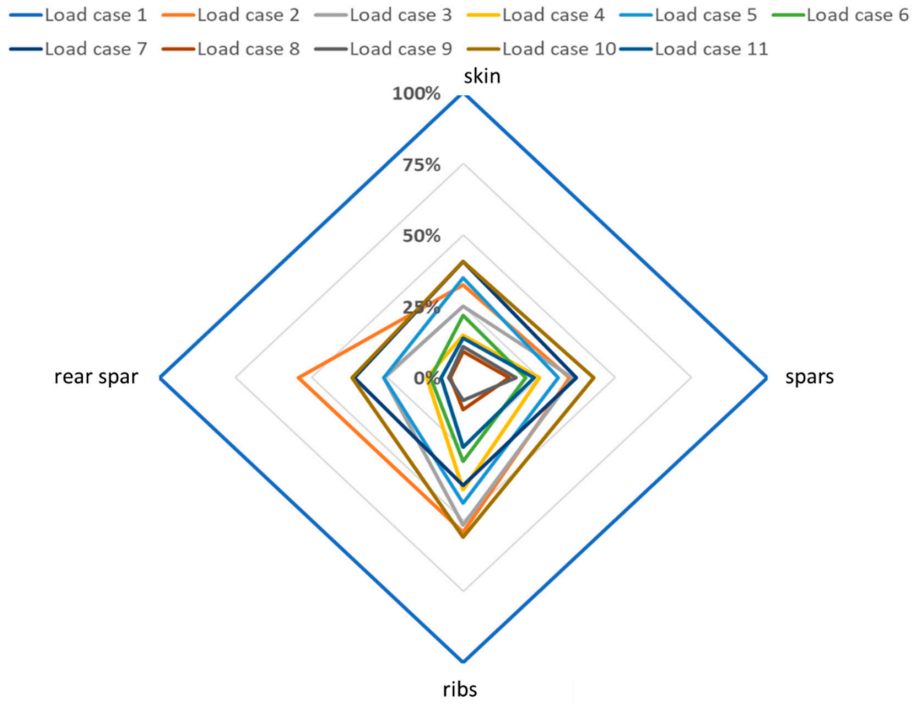

Figure 3. Load case comparison in terms of normalized stress level for the main subparts of the structure.

The skin subpart exhibited the highest level of stress: a peak has been noticed on the upper zone of the skin, close to the cap of the rear spar, leading to a stress concentration. It has been just this outcome to justify the investigation hereafter presented.

2. Criticalities and Approach

The just mentioned stress concentration has occurred on the zone highlighted in Figure 4, depicting the stress map for the aforementioned load case 1. This stress distribution has been assumed as the standard reference load (RL). The type of solicitation is in line with the bending action of the load case, that produces a compression of the skin in span direction and its bending around the spar cap along the chord. This, jointly to the dramatic variation of the local thickness (passing from the overlap of the skin laminate and the cap to the skin alone), can justify the stress concentration.

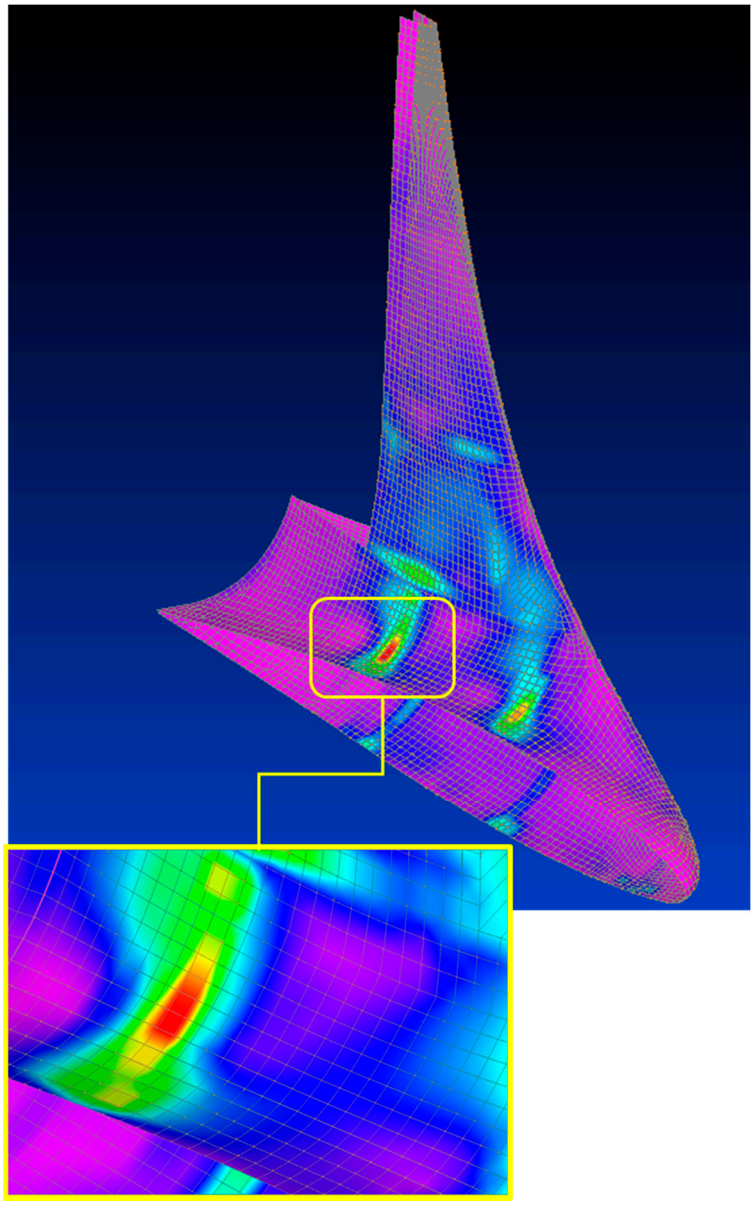

Figure 4. Stress concentration on the upper zone of the skin, close to the rear spar.

However, it is questionable whether the discretization could have a role on the estimate of the stress level. To answer this question a parametric study has been organized, considering progressive refinement levels of the mesh on the zone of interest. This skin

region, as shown in Figure 5, is constituted by two consecutive lines of seven 19 × 19 mm plate elements, towards the span direction. It covers the skin part upstream the spar cap and corresponds to the critical zone highlighted in Figure 4.

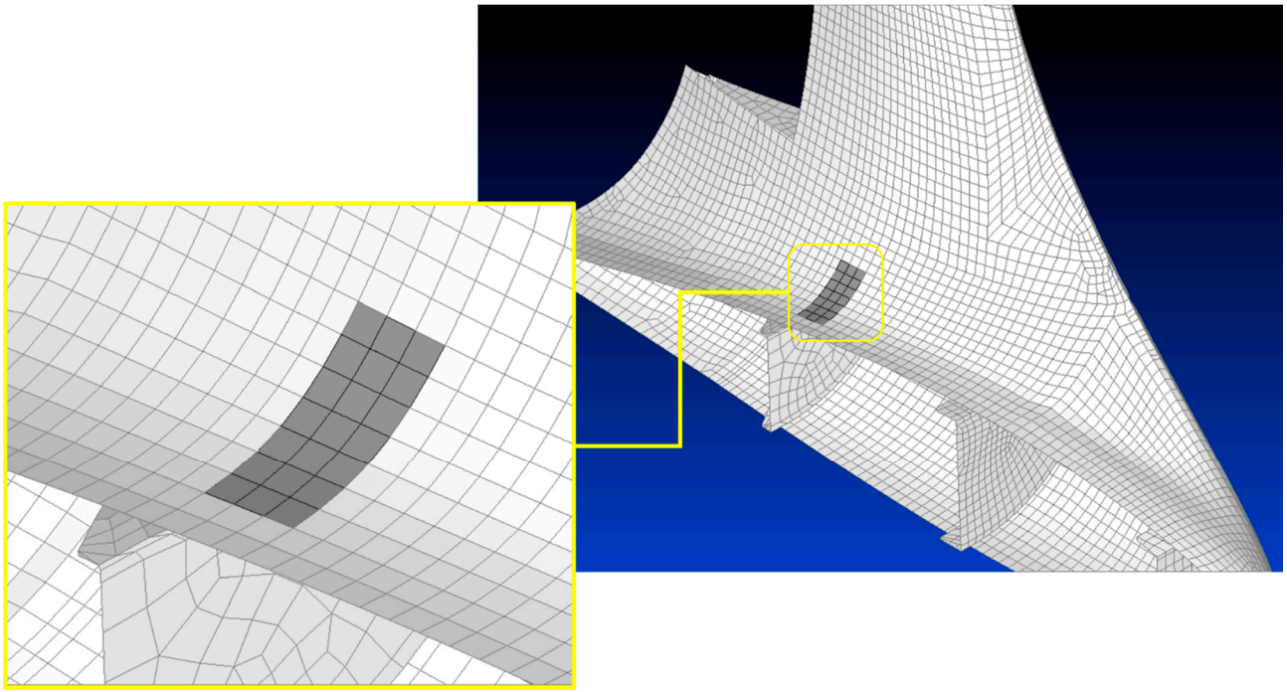

Figure 5. Zone of the model considered for the parametric refinement.

At first, the elements have been split along the chord, since the highest stress gradient occurs along this direction. Then a further split has been performed along the spar, obtaining again square elements. This process -split along the chord and then along the span- has been repeated for two times, coming to the end to square elements 1/4 sized with respect to the original ones. To guarantee an adequate continuity with respect to the surrounding mesh, the boundary elements have been suitably split into triangles, fitting the nodes on the edges.

The stress maps illustrated in Figure 6 show the effect of the level of refinement in terms of stress and distribution. The maximum normalized stress obtained has been summarized in Table 1 and plotted in Figure 7.

Table 1. Maximum normalized stress vs. mesh refinement level; normalization reference: maximum stress computed on the standard reference load (RL) distribution reported in Figure 4.

Case ID	Element Size (mm)	Normalised Stress (%)
reference	19 × 19	100.0
case a	19 × 9.5	107.3
case b	9.5 × 9.5	97.3
case c	9.5 × 4.75	130.9
case d	4.75 × 4.75	154.5

(*) The second dimension refers to the chord direction.

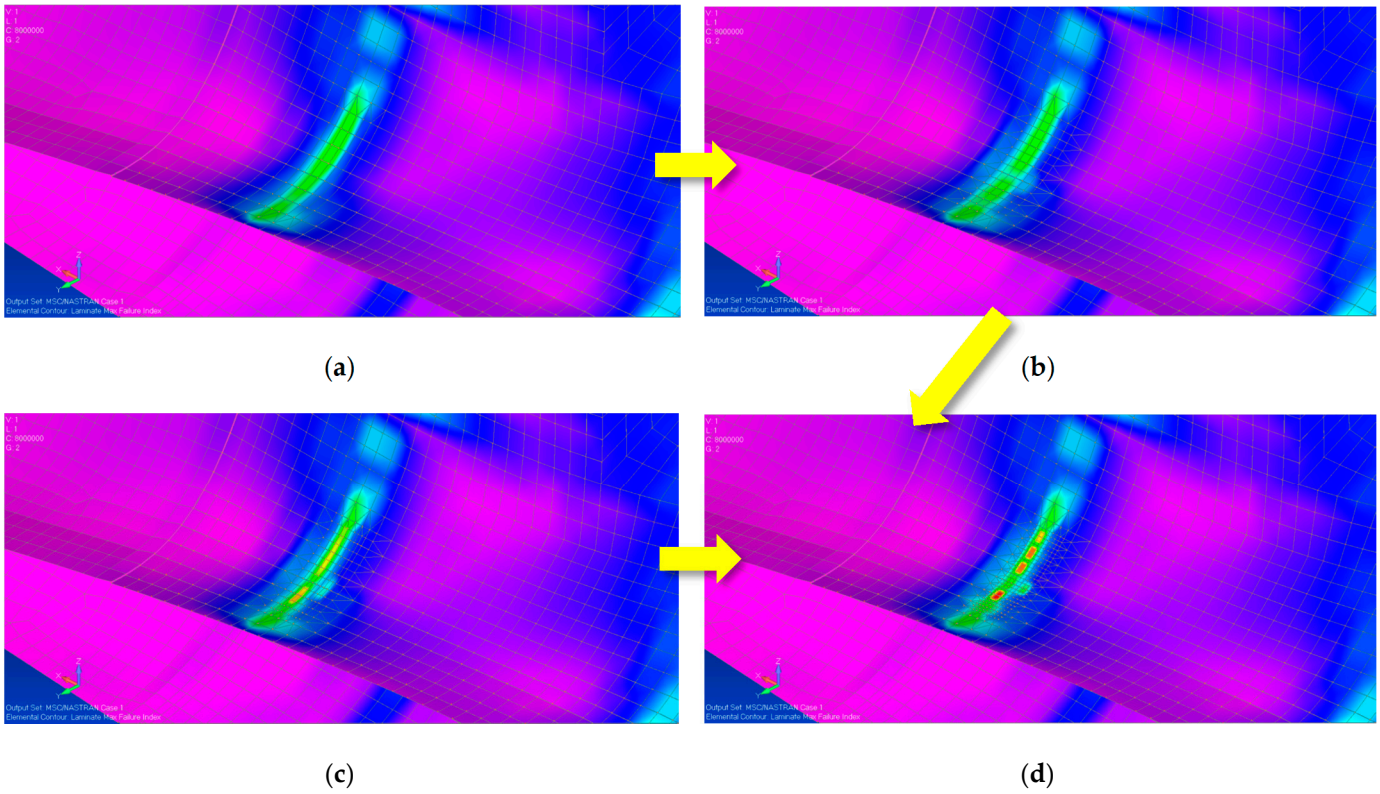

Figure 6. Normalized stress maps vs. mesh refinement level: 1st chordwise split (**a**), 1st spanwise split (**b**), 2nd chordwise split (**c**), 2nd spanwise split (**d**); normalization reference: maximum stress computed on the stress distribution reported in Figure 4 (RL).

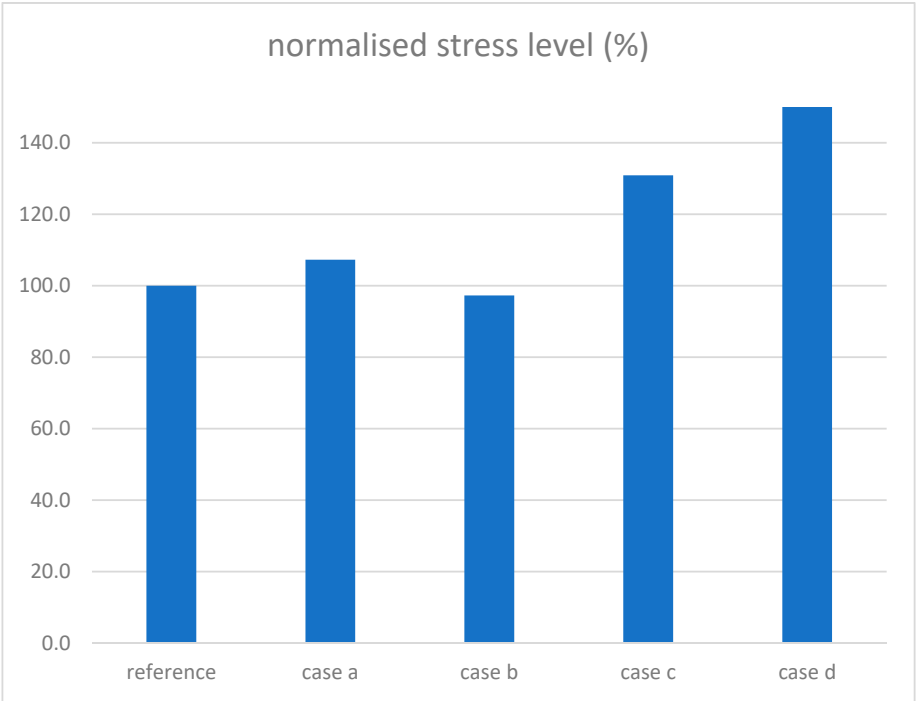

Figure 7. Normalized maximum failure index vs. mesh refinement level: 1st chordwise split (**a**), 1st spanwise split (**b**), 2nd chordwise split (**c**), 2nd spanwise split (**d**); normalization reference: maximum stress computed on the distribution reported in Figure 4 (RL).

The refinement process highlighted, in general, an increasing trend in terms of stress level. This can be explained considering two numerical aspects. The first one is represented by the strain definition as ratio (gradient) of the local displacement over the element size: as this latter term goes to zero over a certain threshold, the division badly handled by the solver. The second aspect is strictly related to the inversion of the structural matrix, whose conditioning level is dramatically affected by its size. This aspect, for the specific case under investigation, however, does not play a fundamental role, since the increase of DOFs due to the local refinement is really modest with respect to the original size of the structural matrix.

The stress maps of the different cases show a concentration on the central part of the investigated zone, with a uniform distribution on the transition between the central zone and the rest of the model. This in some way resizes any mesh boundary effect and focuses the attention on the central part, affected by the discontinuity of stiffness. Another interesting aspect is the impact of both the in-plane element dimension onto the stress. The cases in Figure 6b–d, in fact, show a linear trend punctuated by progressive halving of both the thickness gradient and the in-plane normal directions. This suggests that both the thickness variation and the element size play a role on the observed behavior.

The high level of stress, jointly to the uncertainty related to the just mentioned trend with the refinement of the mesh has led to the adoption of a design solution to mitigate the local accumulation of stress.

As already discussed, the investigated load case determines the inward bending of the winglet, with a consequent compression of the top skin along the span direction. A secondary effect is the bending of the skin also in chordwise direction, between the rear and the middle spars. Considering that the stiffness is higher in the spanwise direction for the overlap of the cap and of the skin laminate and that a sudden variation of rigidity occurs upstream the rear spar, solutions altering the chordwise stiffness look more appropriate. In line with this consideration, a "T" shaped beam bonded on the inner surface of the skin and linking the rear to the middle spar has been investigated. The layout considered is illustrated in Figure 8.

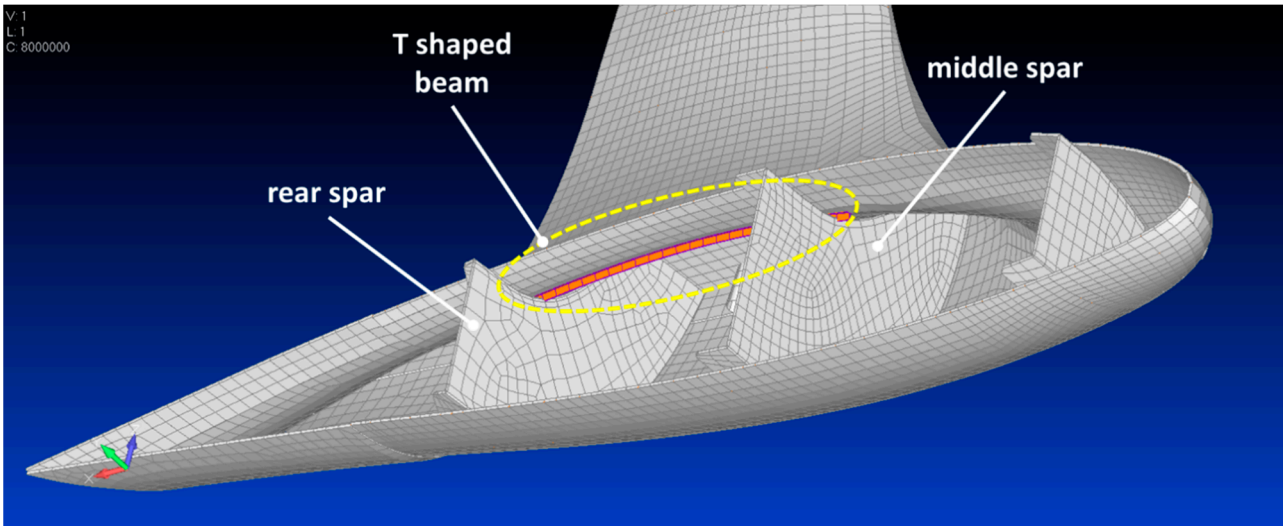

Figure 8. Layout of the chordwise beam to increase the rigidity on the critical zone.

The solution has proved to reduce of about 37% the stress level, thus definitely mitigating the local criticality. A comparison of the initial and final configuration is presented in Figure 9, that highlights a better situation not only on the rear spar but also on the middle spar.

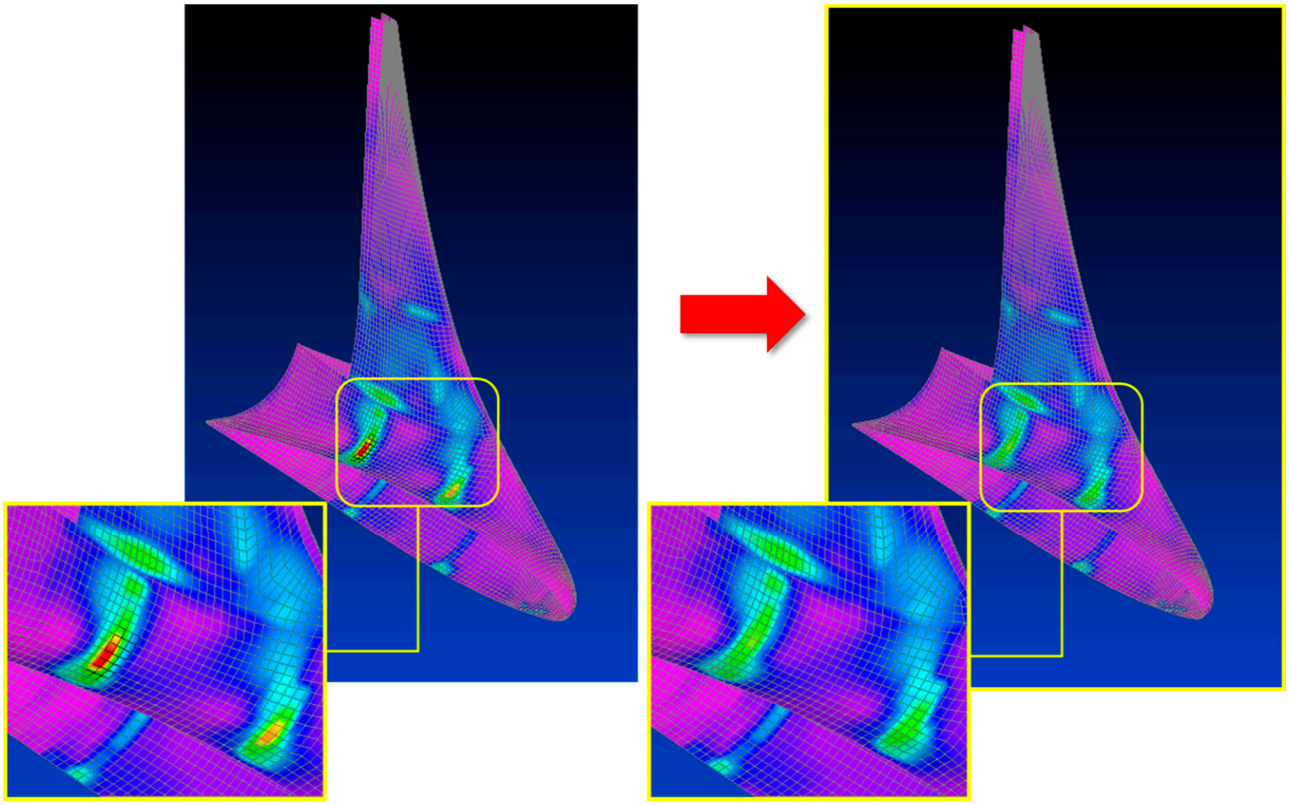

Figure 9. Normalized stress for the original configuration, RL, (**left**) and the one integrated with the additional beam (**right**); normalization reference: maximum stress computed on the distribution reported in Figure 4 (RL).

3. Impact, Discussion and Perspective Works

The just mentioned investigations in some way highlight two aspects that concur to make critical the zone of the skin explored: the sudden and dramatic variation of the local thickness, due to the sudden overlap of the spar-cap to the skin, and the level of discretization adopted to model the zone. The behavior shown by the model leads to severe consideration on its reliability and on the exploitation of the achieved results.

The reliability problem should be faced in two steps: firstly, confining the portion of the model that can be considered computationally robust and, secondly, defining a strategy of elaboration of the results on the critical zone. A model completely refined could help support the first step, in some way confirming the accuracy of the predictions on a certain portion of the winglet domain. A dedicated strategy, on the contrary, should be identified for the second step. Here, the just mentioned concurring aspects (mesh refinement level and thickness variation) should be accurately weighted, jointly to the type of connection between the skin and the spar cap (rigidly or elastically linked, or seen as a unique layup) and, most importantly, the way the load fluxes distribute against the cross-section areas. This last point seems to be the nearest to the physics and suggests a real concentration of stress in the zone; however, the spike due to the thickness discontinuity, further confirmed and emphasized by the sharper and sharper gradient of progressive mesh refinements, should be realistically interpreted and smoothed by means of a moving average process. The plot of Figure 10 illustrates the effect of a moving average three-element windowed, on the FI computed critical strip highlighted in Figure 2. A remarkable mitigation of about 55% on the rear spar has been estimated. In any case, experimental information coming from strain gage local measurements, discussed in the next section should drive or at least support the reliability process of the model.

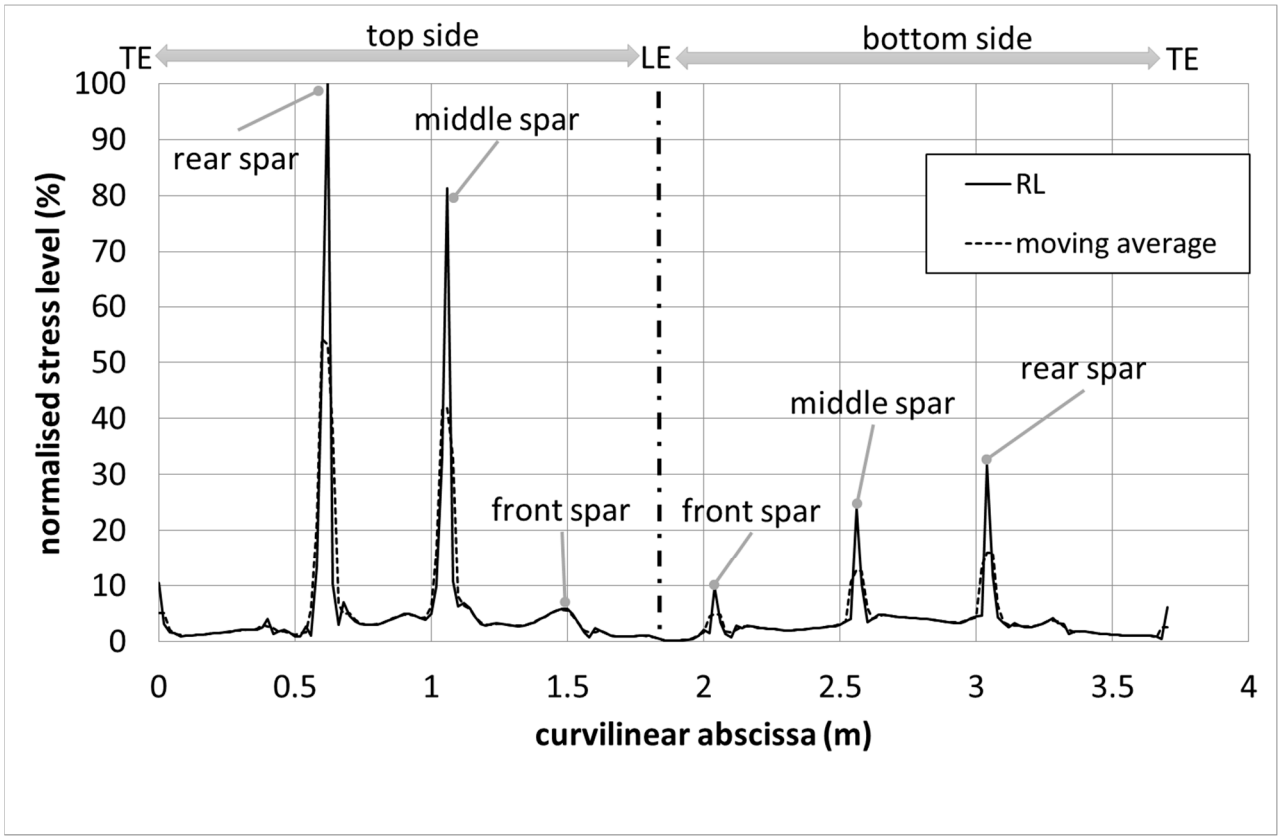

Figure 10. Normalized stress level vs. curvilinear abscissa of the winglet strip: original (solid) and after moving average (dashed); normalization reference: maximum stress computed on the distribution reported in Figure 4 (RL).

These issues suggested the investigators to move towards slightly different and more robust numerical configurations, that avoided the insurgence of those spikes.

4. Experimental Issues

The envisaged singularities were so defined mainly for their very limited, almost point extension. Even considering this characteristic can be hardly linked to a physical behavior, we cannot attribute this result to a pure mathematical issue. Conversely, it is very hard to reveal that behavior experimentally, and should it be not found, the doubt remains concerning its existence or not: is it the net sufficiently narrow to catch that small peak? This consideration leads to important consequences. Strain gauges are not appropriate to further investigate the phenomenon. They are significantly wider than the area of interest, and they have the bad characteristic integrated into the info over their area, so that a mean value is actually detected. Furthermore, their installation could somehow affect the measurements in itself, just for their finite area. A good alternative could be represented by the use of distributed fiber optics, that can exhibit very dense measurement arrays, stepped and extended a few mm. In that case, however, it should be considered that the measure could only be directional, while a 2D field could be acquired with an appropriate and well-defined deployment. Hand placement does not favor the accuracy of measures on very specific areas. Even more, the numerical results would suggest the need of an accurate investigation "by the single layers" of the composite structure. This further complexity could indeed be solved by embedding the thin fibers within several layers, at least in principle. Other methods of investigation could be also exploited, as for instance accurate laser map measurements, that has however the backlash of needing numerical derivation to attain strain information, with the further complexity that the structure is not slender and that the measured displacement is normal to the requested longitudinal strain.

The conclusion is that this kind of phenomena deserves dedicated investigations to be faced and finally solved. Available technology seems to provide some opportunities. Nevertheless, the test campaign shall be designed very accurately since the beginning to allow a certain level of success. An almost obvious, further consideration is that the reference object itself should be properly designed in order to match numerical and physical requirements, and be relevant on the investigation point of view.

5. Conclusions and Further Steps

The abovementioned results, and the surrounding conditions that they were obtained from, give a lot of interesting keys for further deepening of this kind of analysis.

First of all, as cited in the introduction, these kinds of meshes and the complex architecture is almost a constant for morphing systems; which means that this situation is doomed to be recurrent for this kind of modeling, irrespectively of the adopted configuration. Therefore, it is worthy of study and should be understood in detail.

The obvious consequence is that these kinds of outcomes will repeat more or less equally for the different architectures, so that a recursive impact on design and verification times is expected—then propagating to the development times.

The reported issue is not dramatic in itself, even if it should reveal to be coherent with the physical behavior, as it was shown that minimal intervention on the structural architecture may report the strain excess to usual and controllable values. Additionally, the effectiveness of that solution itself—directly affecting the local stiffness and in some way mitigating the discontinuity of rigidity—supports the hypothesis of a stress concentration due to the sudden variation of thickness. Indeed, the thickness variation has a relevant impact upon the stiffness matrix, due to the cubic dependence.

For the statement above, it could be argued that this issue could be eliminated by a simple implementation of minor adjustments, affecting the layout and the weight, minimally. The easy answer is that once the bug has been pointed out, it is safe to adequately investigate the problem, to avoid further, dramatic consequences in successive design processes.

Even if these outcomes should prove to be far from design reality, it could be speculated that they are signals of some specific structural modality behavior, which could emerge as some damage or discontinuity occurs (for instance, as the effect of an impact of simple aging). The area of interests should be then regarded as a "hot spot", worthy of monitoring along the system lifetime. In this case, the inclusion of embedded fibers shall be relevant for a continuous strain levels monitoring under operational loads at ground (a very basic, but perhaps effective SHM system).

As experimental campaigns should be designed very carefully, in order to properly characterize the phenomenon under investigation, in the same way numerical investigations activity could be structured and detailed in order to attain specific information and possibly, relevant solutions.

Author Contributions: Conceptualization, S.A., I.D. and L.P.; methodology, S.A., I.D. and A.C.; software, S.A.; validation, A.C. and U.M.; formal analysis, L.P.; investigation, L.P. and I.D.; resources, U.M.; data curation, L.P.; writing—original draft preparation, S.A.; writing—review and editing, I.D. and A.C.; visualization, A.C.; supervision, U.M.; project administration, U.M.; funding acquisition, U.M. All authors have read and agreed to the published version of the manuscript.

Funding: This research was funded by Clean Sky 2 Joint Undertaking, under the European's Union Horizon 2020 research and innovation Programme, under grant agreement No 807089—REG GAM 2018—H2020-IBA-CS2- GAMS-2017.

Institutional Review Board Statement: Not applicable.

Informed Consent Statement: Not applicable.

Data Availability Statement: Not applicable.

Acknowledgments: The AirGreen2 Project has received funding from the Clean Sky 2 Joint Undertaking, under the European's Union Horizon 2020 research and innovation Programme, under grant agreement No 807089—REG GAM 2018—H2020-IBA-CS2- GAMS-2017.

Conflicts of Interest: The authors declare no conflict of interest.

Abbreviations

A/C	Aircraft
CFD	Computational Fluid Dynamics
CS2	Clean Sky 2 Programe
CFRP	Carbon Fiber Reinforced Polymer
CL	Lift coefficient
DOF	Degree of Freedom
FE	Finite Element
FEM	Finite Element Model
GRA	Green Regional Aircraft
LCA	Load Control and Alleviation
LDO	Leonardo Aircraft Division
LE	Leading Edge
LoD	Lift over Drag
RL	Standard Reference Load
SDOF	Single Degree of Freedom
SHM	Structural Health Monitoring
TE	Trailing Edge
UD	Unidirectional

References

1. Ameduri, S.; Concilio, A.; Dimino, I.; Pecora, R.; Ricci, S. AIRGREEN2—Clean Sky 2 Programme: Adaptive Wing Technology Maturation, Challenges and Perspectives. In Proceedings of the ASME 2018 Conference on Smart Materials, Adaptive Structures and Intelligent Systems, San Antonio, TX, USA, 10–12 September 2018. [CrossRef]
2. Peter, F.; Stumpf, E. The development of morphing aircraft benefit assessment. In *Morphing Wing Technologies, Large Commercial Aircraft and Civil Helicopters*; Concilio, A., Dimino, I., Lecce, L., Pecora, R., Eds.; Butterworth-Heinemann: Oxford, UK, 2018; Volume 3, pp. 103–121.
3. Kota, S.; Osborn, R.; Ervin, G.; Maric, D. Mission adaptive compliant wing–design, fabrication and flight test. In Proceedings of the NATO Research Technology Organization Research Symposium, Morphing Vehicles, RTO-MP-AVT-168 2009, Evora, Portugal, 20–24 April 2009.
4. NASA; US AFRL. Adaptive compliant trailing edge flight experiment. *RC Soar. Digest* **2014**, *31*, 85–86.
5. Herrera, C.Y.; Spivey, N.D.; Lung, S.F.; Ervin, G.; Arbor, A.; Flick, P. Aeroelastic airworthiness assessment of the adaptive compliant trailing edge flaps. In Proceedings of the 46th Society of Flight Test Engineers International Symposium, Lancaster, CA, USA, 14–17 September 2015.
6. Radestock, M.; Riemenschneider, J.; Monner, H.P.; Rose, M. Experimental investigation of a compliant mechanism for an uav leading edge. In Proceedings of the 7th Eccomas Thematic Conference on Smart Structures and Materials, Smart 2015, Azores, Portugal, 3–6 June 2015.
7. Arena, M.; Amoroso, F.; Pecora, R.; Amendola, G.; Dimino, I.; Concilio, A. Numerical and experimental validation of a full scale servo-actuated morphing aileron model. *Smart Mater. Struct.* **2018**, *27*, 105034. [CrossRef]
8. McGowan, A.-M.R.; Vicroy, D.D.; Busan, R.C.; Hahn, A.S. Perspectives on Highly Adaptive or Morphing Structures. In Proceedings of the NATO Research Technology Organization Applied Vehicle Technology Panel Symposium, RTO-MP-AVT-152 2009, Evora, Portugal, 20–24 April 2009.
9. Chattopadyay, N.C.; Jony, B.; Acharya, A. An analysis on wing morphing. In Proceedings of the Global Engineering, Science and Technology Conference 2012, Dhaka, Bangladesh, 28–29 December 2012.
10. Delery, J.; Fulker, J.; de Matteis, P. *Drag Reduction by Shock and Boundary Layer Control: Results of the Project Euroshock II, Supported by the European Union 1996–1999, Notes on Numerical Fluid Mechanics and Multidisciplinary Design*; Springer Science & Business Media: Berlin/Heidelberg, Germany, 2013; Volume 80, ISBN 978-3-540-45856-2.
11. Stanewsky, E.; Delery, J.; Fulker, J.; Geissler, W. Euroshock-Drag Reduction by Passive Shock Control: Results of the Project Euroshock, AER2-CT92–0049, Supported by the European Union, 1993–1995. In *Notes on Numerical Fluid Mechanics*; Springer Science & Business Media: Berlin/Heidelberg, Germany, 2013; Volume 56, ISBN 978-3-322-90711-0.
12. Ameduri, S.; Concilio, A. Morphing wings review: Aims, challenges, and current open issues of a technology. *Proc. Inst. Mech. Eng. Part C J. Mech. Eng. Sci.* **2020**. [CrossRef]

13. Fleming, G.A.; Burner, A.W. Deformation measurements of smart aerodynamic surfaces. In Proceedings of the SPIE Conference on Optical Diagnostics for Fluids/Heat/Combustion and Photomechanics for Solids, Denver, CO, USA, 21–23 July 1999.
14. Ameduri, S.; Ciminello, M.; Concilio, A.; Brindisi, A.; Petrella, O.; Tiseo, B.; Mazzola, L.; Piscitelli, F.; Sorrentino, R. Design approach of a large strain sensor based on nanoparticle technology: A highly-integrable sensor for Morphing applications including SHM & shape reconstruction. In Proceedings of the 2017 13th Conference on Ph.D. Research in Microelectronics and Electronics (PRIME), Taormina, Italy, 12–15 June 2017.
15. Romano, F.; Barile, M.; Cacciapuoti, G.; Godard, J.L.; Vollaro, P.; Barabinot, P. Advanced OoA and Automated Technologies for the Manufacturing of a Composite Outer Wing Box. In Proceedings of the 8th EASN-CEAS International Workshop on Manufacturing for Growth and Innovation, Glasgow, UK, 4–7 September 2018; pp. 1–8. [CrossRef]
16. Available online:. Available online: https://www.compositesworld.com/articles/multilayer-thermoplastic-tapes-afp-and-resin-infusion-for-more-democratic-composites (accessed on 13 March 2021).
17. Moens, F. Augmented Aircraft Performance with the Use of Morphing Technology for a Turboprop Regional Aircraft Wing. *Biomimetics* **2019**, *4*, 64. [CrossRef] [PubMed]
18. de Gaspari, A.; Cavalieri, V.; Ricci, S. Advanced Design of a Full-Scale Active Morphing Droop Nose. *Int. J. Aerosp. Eng.* **2020**, *2020*, 1086518. [CrossRef]
19. Rea, F.; Amoroso, F.; Pecora, R.; Noviello, M.C.; Arena, M. Structural design of a multifunctional morphing fowler flap for a twin-prop regional aircraft. In Proceedings of the ASME 2018 Conference on Smart Materials, Adaptive Structures and Intelligent Systems, San Antonio, TX, USA, 10–12 September 2018. [CrossRef]
20. Fonte, F.; Toffol, F.; Ricci, S. Design of a Wing Tip Device for Active Maneuver and Gust Load Alleviation. In Proceedings of the AIAA/ASCE/AHS/ASC Structures, Structural Dynamics, and Materials Conference—AIAA SciTech, Kissimmee, FL, USA, 8–12 January 2018; pp. 1–18, ISBN 9781624105326. [CrossRef]
21. Amendola, G.; Dimino, I.; Concilio, A.; Pecora, R.; Cascio, M.L. Preliminary Design Process for an Adaptive Winglet. *Int. J. Mech. Eng. Robot. Res.* **2018**, *7*. [CrossRef]
22. Dimino, I.; Amendola, G.; Di Giampaolo, B.; Iannaccone, G.; Lerro, A. Preliminary design of an actuation system for a morphing winglet. In Proceedings of the 8th International Conference on Mechanical and Aerospace Engineering (ICMAE), Prague, Czech Republic, 22–25 July 2017; pp. 416–422. [CrossRef]
23. Dimino, I.; Andreutti, G.; Moens, F.; Fonte, F.; Pecora, R.; Concilio, A. Integrated Design of a Morphing Winglet for Active Load Control and Alleviation of Turboprop Regional Aircraft. *Appl. Sci.* **2021**, *11*, 2439. [CrossRef]
24. Dimino, I.; Gallorini, F.; Palmieri, M.; Pispola, G. Electromechanical Actuation for Morphing Winglets. *Actuators* **2019**, *8*, 42. [CrossRef]
25. Noviello, M.C.; Dimino, I.; Concilio, A.; Amoroso, F.; Pecora, R. Aeroelastic Assessments and Functional Hazard Analysis of a Regional Aircraft Equipped with Morphing Winglets. *Aerospace* **2019**, *6*, 104. [CrossRef]